

# CHAPTER I

## INTRODUCTION

### 1.1 INTRODUCTION TO NANOTECHNOLOGY

Science and technology are now so intertwined in our lives that they are causing massive shifts in all fields of technical knowledge. As these new advances make their way into actual applications, they open up new possibilities [1]. The twentieth century was regarded as the century of physical sciences, whereas the twenty-first century was regarded as the century of life sciences. However, nanoscience is a new discipline of science that unifies both physical and life sciences and will revolutionise our understanding of science and technology in the twenty-first century. Nanoscience and nanotechnology are founded on our ability to measure, manipulate, and organize materials at the nanoscale, which is a billionth of a metre ( $10^{-9}$ m). Nanotechnology is the manipulation and rearrangement of matter at the atomic and molecular level in order to produce new materials, gadgets, and functioning systems [2].

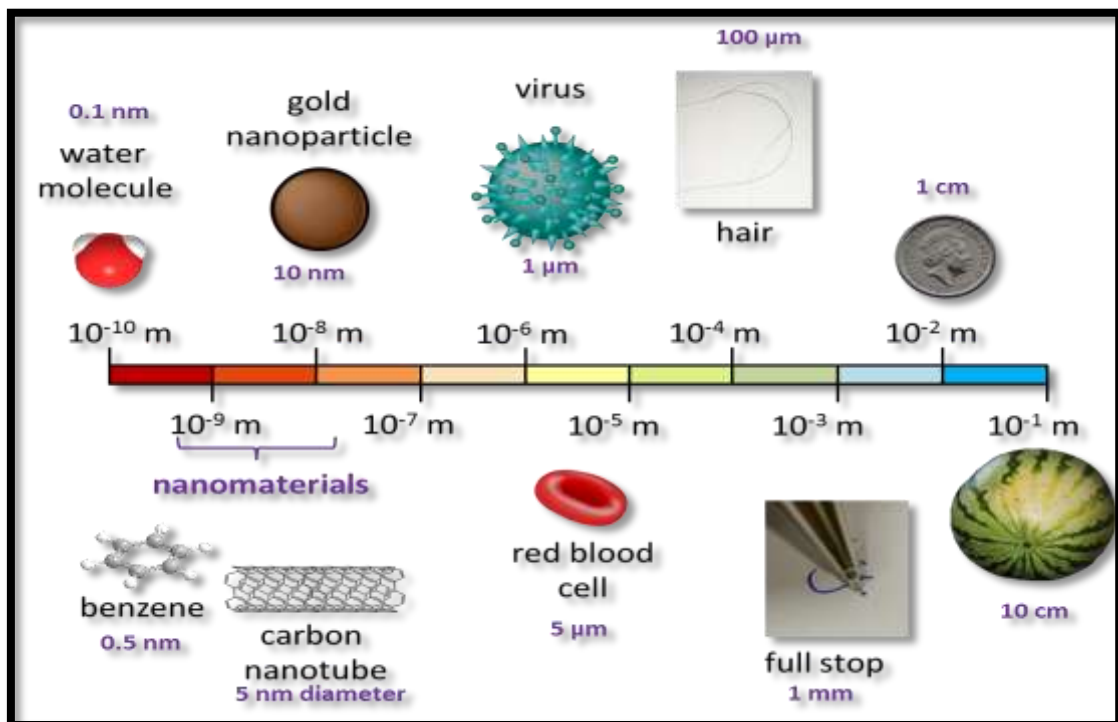



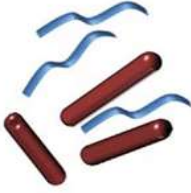
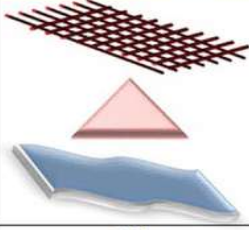
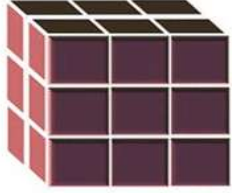
Figure 1.1 Nano scale and Nanostructure

New enhanced and potentially helpful nano methods are generated by integrating nanoscience and technology. Figure 1.1 depicts a nanoscale and nanotechnology image. Many individuals are interested in nanotechnology because nanoscale materials offer unique properties that could lead to a slew of new technological applications [3]. The scope of developing new knowledge to explain the size-dependent growth of diverse physical properties, previously undetected features, and other phenomena is expanding. Within the empirical discipline of nanotechnology, various basic and applied scientific disciplines have been quickly encapsulated. It has recently emerged as one of the most important fields, with the ability to improve existing technologies' efficiency and outcomes. Nanotechnology holds a lot of promise for presenting us with many breakthroughs in the future that will shift the course of technical progress in a variety of fields [4]. Nanotechnology will undoubtedly have a significant impact in fields such as electronics, communication, medical devices, medicine, cosmetics, architecture, textile, agricultural, food, metallurgy, defence and security, space, and many others.

The technology has huge potential in the medical, pharmaceutical, biotechnology, engineering, manufacturing, telecommunications, and information technology industries. It will have a broad and far-reaching impact in many domains, not just in terms of cost effectiveness and performance gains over current products and processes, but also in the long run, yielding innovative approaches to health and societal problems. The synthesis, characterization, exploration, and use of nanostructured materials are all part of nanotechnology. Nanostructured materials are fascinating for a variety of reasons, both scientific and practical [5].

## **1.2 NANOMATERIALS**

Nanomaterials are chemical compounds made and used on a very small scale. These materials were created to have unique properties as compared to bulk materials. A group of substances known as a nanomaterial has at least one dimension of less than 100 nanometers and Figure 1.2 shown the images of Nanomaterials. The diameter of a human hair is 100,000 times smaller than a nanometer, which is equal to  $10^{-9}$ m. Nanomaterials are fascinating because they exhibit unique optical, magnetic, electrical, and other properties at such a small scale.

Isotropic nanomaterials		Anisotropic nanomaterials	
			
<b>0D</b>	<b>1D</b>	<b>2D</b>	<b>3D</b>
<b>Spheres, Clusters</b>	<b>Nanorods, wires</b>	<b>Nanofilms, plates</b>	<b>Nanoparticles</b>

**Figure 1.2 Types of Nanomaterials**

### **Zero-dimensional nanomaterials**

Zero-dimensional materials are materials wherein all the dimensions are measured within the nanoscale (no dimension).

### **One-dimensional nanomaterials**

One-dimensional nanomaterials are ideal systems for exploring a number of new phenomena at the nanoscale and investigating the size and dimensionality dependence of functional properties. They are also expected to play an important role as both interconnects and the key units in fabricating electronic optoelectronic and light-emitting diodes (LEDs) with nanoscale dimensions.

### **Two-dimensional nanomaterials**

Dimensions of two are not confined to the nanoscale; two dimensional nanomaterials exhibit plate-like shapes. It includes nanofilms, nanolayers, and nanocoatings, etc [6,7].

### **Three-dimensional nanomaterials**

Three-dimensional nanomaterials are materials which are characterised by having three arbitrary dimensions above 100 nm. These materials possess a nanocrystalline structure.

## **1.3 SYNTHESIS OF NANOPARTICLES**

The nanoparticles are synthesised in a manner in which the resulting nanoparticles must have the following properties:

- Identical in size
- Identical in shape
- Identical in chemical composition and crystal structure
- Individually dispersed with no agglomeration

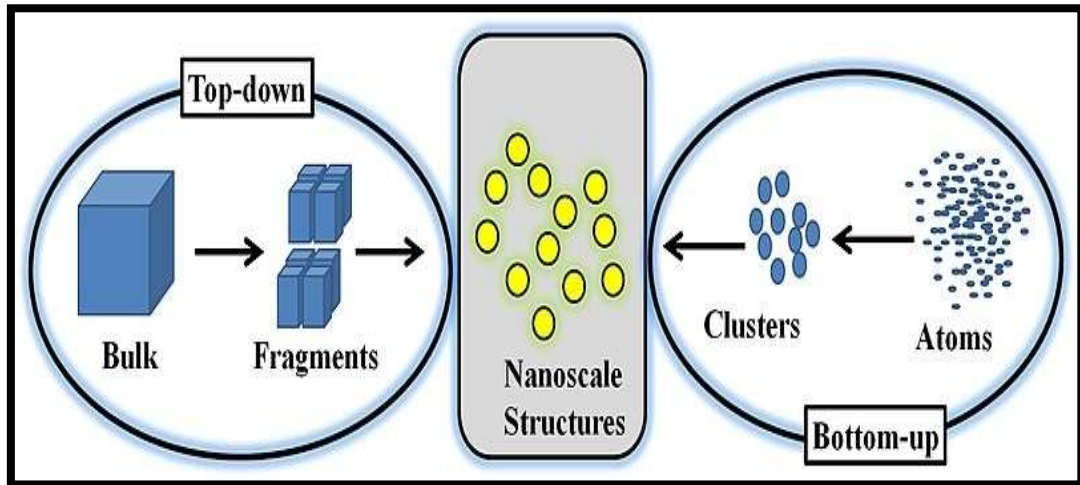
### **1.3.1 Top Down Approach**

The bulk material is broken down into nanosized structures or particles in a top-down method. Top-down synthesis techniques are an evolution of those used to create micron-sized particles which is showed in Figure 1.3. Top-down techniques are naturally simpler, relying on bulk material removal or division, or bulk fabrication process downsizing, to produce the required structure with sufficient attributes. The most prevalent top-down fabrication approach is nanolithography. To obtain the desired structure, the needed material is first shielded by a mask, and then the exposed material is etched away [8]. Depending on the resolution level necessary for features in the final product, etching of the base material can be done chemically with acids or mechanically with ultraviolet light, X-rays, or electron beams. This method is also used in the production of computer chips.

### **1.3.2 Bottom Up Approach**

The 'bottom-up' strategy is an alternative that has the potential to produce less waste and hence be more cost-effective. The atom-by-atom, molecule-by-molecule, or cluster-by-cluster construction of a material is referred to as a bottom-up approach. Many of these approaches are still under development or are only now being employed for commercial nanopowder manufacture [9].

The bottom-up method is also inspired by biological systems, where nature has used chemical forces to generate virtually all of the structures required for existence. The goal is to duplicate nature's ability to make small clusters of certain atoms that can subsequently self-assemble into more complex structures [10].



**Figure 1.3 Top-down and Bottom-up approach**

#### **1.4 PROPERTIES OF NANOMATERIALS**

Nanomaterials have the structural features in between of those of atoms and the bulk materials. While most microstructure materials have similar properties to the corresponding bulk materials, the properties of materials with nanometre dimensions are significantly different from those of atoms and bulks materials. This is mainly due to the nanometre size of the materials which render them

- Large fraction of surface atoms
- High surface energy
- Spatial confinement
- Reduced imperfections, which do not exist in the corresponding bulk materials

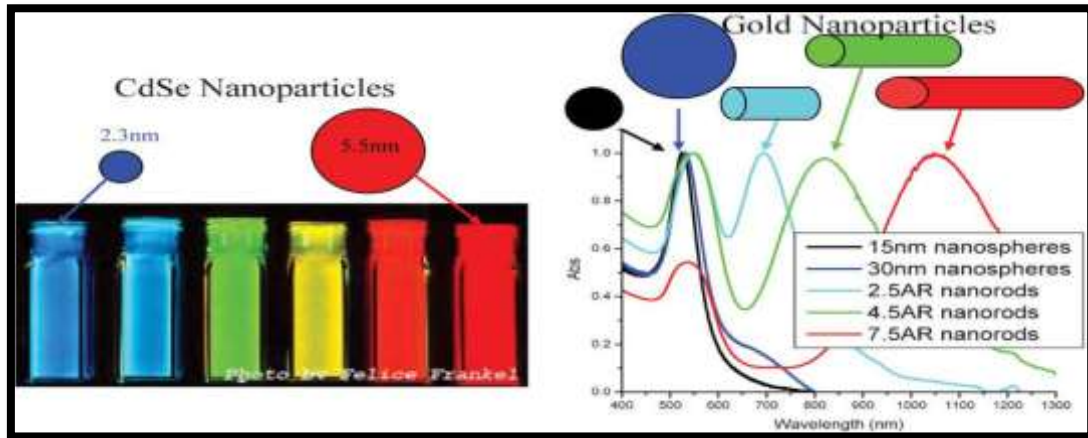
Nanomaterials have an unusually large surface area to volume ratio because to their short dimensions, leading in a large surface or interfacial atoms, resulting in more "surface" dependant material characteristics [11]. The surface properties of nanoparticles will affect the entire material, especially when the sizes of nanomaterials are comparable to length. As a result, the bulk materials' qualities may be enhanced or modified. Metallic nanoparticles, for example, can be used as highly active catalysts. The sensitivity and selectivity of chemical sensors made from nanoparticles and nanowires were improved [12]. Nanomaterials with nanoscale

feature sizes have a spatial confinement effect on the materials, resulting in quantum phenomena.

The energy band structure and charge carrier density in the materials can be changed in a different way than in their bulk, which affects the materials' electrical and optical properties. Lasers and light emitting diodes (LED) made from quantum dots and quantum wires, for example, are particularly promising in future optoelectronics. Quantum dot technologies for high-density data storage are likewise a rapidly expanding field. Reduced defects play a significant role in determining the characteristics of nanomaterials. Impurities and intrinsic material flaws will shift to near the surface during thermal annealing, which supports a self-purification process. The properties of nanoparticles are affected by this increasing material perfection. For example, chemical stability for particular nanoparticles may be improved, and nanomaterials' mechanical qualities will be superior to bulk materials. Carbon nanotubes have outstanding mechanical characteristics.

#### **1.4.1 Optical Properties**

The optical characteristics of nanoparticles are one of the most exciting and valuable elements of them. Optical detectors, lasers, sensors, imaging, phosphors, displays, solar cells, photo catalysis, photo electrochemistry, and biomedicine are some of the applications based on optical features of nanomaterials. Nanomaterials' optical properties are influenced by factors such as feature size, shape, surface characteristics, and other factors such as doping and contact with the environment or other nanostructures. Similarly, the shape of metal nanostructures can have a significant impact on their optical characteristics. The difference in optical characteristics of metal and semiconductor nanoparticles is illustrated in Figure. The optical characteristics of CdSe semiconductor nanoparticles can be changed simply by changing their size and showed in Figure 1.4. As seen in the several samples of gold nanospheres, when metal nanoparticles are enlarged, their optical characteristics vary only slightly. However, when an anisotropy is added to the nanoparticle, such as formation of nanorods, the optical characteristics of the nanoparticles alter substantially [13,14].



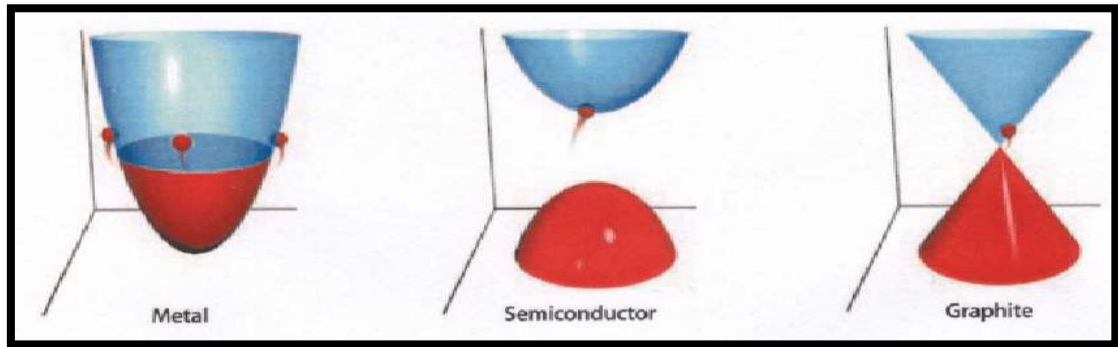
**Figure 1.4 Fluorescence emission of (CdSe) ZnS quantum dots of various sizes and absorption spectra of various sizes and shapes of gold nanoparticles**

### 1.4.2 Structural Properties

Interatomic spacing alters as surface area and surface energy rise with decreasing particle size. This is due to internal pressure caused by the compressive strain causing a tiny radius of curvature in the nanoparticle. The atomic spacing grows as the particle size decreases in semiconductors and metals. Cuboctahedra, icosahedra, tetrahedron, and decahedra are polyhedral structures found in metallic nanoparticles such as gold and silver. These nanoparticles can be thought of as multiply twinned crystalline particles (MTPs), whose forms are explained by the surface energies of different crystallographic planes [15].

### 1.4.3 Electrical Properties

Electrical Properties of nanoparticles mainly focuses about fundamentals of electrical conductivity in nanotubes and nanorods, carbon nanotubes, photoconductivity of nanorods, electrical conductivity of nanocomposites and showed in Figure 1.5. One interesting method which can be used to demonstrate the steps in conductance is the mechanical thinning of a nanowire and measurement of the electrical current at a constant applied voltage. The important point here is that, with decreasing diameter of the wire, the number of electron wave modes contributing to the electrical conductivity because much smaller by well-defined quantized steps [16].



**Figure 1.5 Electrical Properties**

#### **1.4.4 Mechanical Properties**

Mechanical Properties of Nanoparticles deals with bulk metallic and ceramic materials, influence of porosity, influence of grain size, super plasticity, filled polymer composites, particle-filled polymers, polymer-based nanocomposites filled with platelets, carbon nanotube-based composites. That it is problematic to produce macroscopic bodies with a high density and a grain size in the range of less than 100 nm. However, two materials, neither of which is produced by pressing and sintering, have attracted much greater interest as they will undoubtedly achieve industrial importance. These materials are polymers which contain nanoparticles or nanotubes to improve their mechanical behaviours, and severely plastic-deformed metals, which exhibit astonishing properties. However, because of their larger grain size, the latter are generally not accepted as nanomaterials. Experimental studies on the mechanical properties of bulk nanomaterials are generally impaired by major experimental problems in producing specimens with exactly defined grain sizes and porosities. Therefore, model calculations and molecular dynamic studies are of major importance for an understanding of the mechanical properties of these materials. Filling polymers with nanoparticles or nanorods and nanotubes, respectively, leads to significant improvements in their mechanical properties. Such improvements depend heavily on the type of the filler and the way in which the filling is conducted, the latter point is of special importance, as any specific advantages of a Nano particulate filler may be lost if the filler forms aggregates, thereby mimicking the large particles. This depends on the shape of the filler, particles or platelets, and on the degree of agglomeration. In this class of material, polymers filled with silicate platelets exhibit the best mechanical properties and are of the greatest economic relevance [17]. The larger the

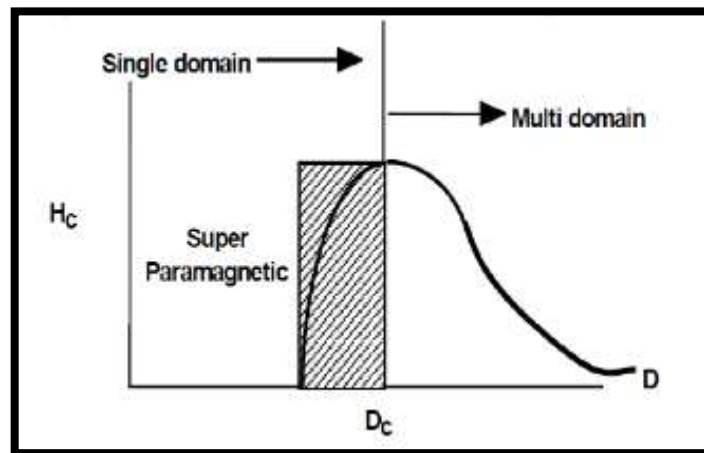


particles of the filler or agglomerates, the poorer are the properties obtained. Although, potentially, the best composites are those filled with nanofibers or nanotubes, because such composites have the least ductility. On the other hand, by using carbon nanotubes it is possible to produce composite fibers with extremely high strength and strain at rupture. Among the most exciting nanocomposites are the polymer-ceramic nanocomposites, where the ceramic phase is platelet-shaped. This type of composite is preferred in nature, and is found in the structure of bones, where it consists of crystallized mineral platelets of a few nanometers thickness that are bound together with collagen as the matrix. Composites consisting of a polymer matrix and defoliated phyllosilicates exhibit excellent mechanical and thermal properties.

#### **1.4.5 Magnetic properties**

Bulk gold and Pt are non-magnetic, but at the nano size they are magnetic. Surface atoms are not only different to bulk atoms, but they can also be modified by interaction with other chemical species, that is, by capping the nanoparticles and Magnetic properties of nanostructured materials are showed in Figure 1.6. This phenomenon opens the possibility to modify the physical properties of the nanoparticles by capping them with appropriate molecules. Actually, it should be possible that non-ferromagnetic bulk materials exhibit ferromagnetic-like behaviour when prepared in nano range. One can obtain magnetic nanoparticles of Pd and Pt from non-magnetic bulk materials. In the case of Pt and Pd, the ferromagnetism arises from the structural changes associated with size effects. However, gold nanoparticles become ferromagnetic when they are capped with appropriate molecules: the charge localized at the particle surface gives rise to ferromagnetic-like behaviour. Surface and the core of Au nanoparticles with 2 nm in diameter show ferromagnetic and paramagnetic character, respectively. The large spin-orbit coupling of these noble metals can yield to a large anisotropy and therefore exhibit high ordering temperatures. More surprisingly, permanent magnetism was observed up to room temperature for thiol-capped Au nanoparticles. For nanoparticles with sizes below 2 nm the localized carriers are in the 5d band. Bulk Au has an extremely low density of states and becomes diamagnetic, as is also the case for bare

Au nanoparticles. This observation suggested that modification of the d band structure by chemical bonding can induce ferromagnetic like character in metallic clusters [18].



**Figure 1.6 Magnetic properties of nanostructured materials.**

#### **1.4.6 Thermal properties**

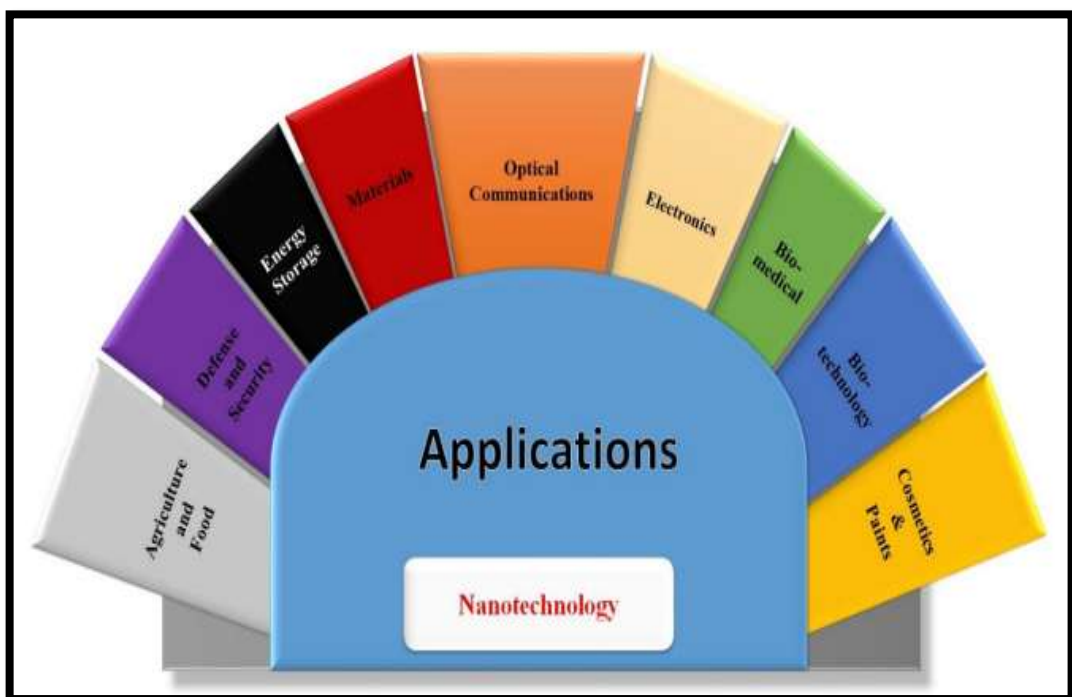
The studies on thermal properties of nanomaterials have seen lower progression due to the difficulties of experimental measuring and controlling the thermal transport in nanoscale dimensions. In order to measure the thermal transport of nanostructures with high spatial resolution, Atomic force microscope (AFM) has been introduced with nanometer scale which provides a promising way to probe the thermal properties with nanostructures. The size, shape and large surface area changes the thermal properties of the nanomaterials which exposes a small different behaviour when compared to the bulk. For example, because of the tubular structures of carbon nanotubes, they have extremely high thermal conductivity in axial directions, leaving high anisotropy in the heat transport in the materials. The interfaces are also a very important factor for determining the thermal properties of nanomaterials [19].

#### **1.4.7 Chemical properties**

Nanoscale structures such as nanoparticles and nanolayers have high surface area to volume ratios that potentially differ in their crystallographic structures and that may lead to radical changes in their chemical reactivity. Nanoparticles often exhibit new chemistry as distinct from their larger particulate counter parts; for example, many new medicines will dissolve easily when it is in nanostructured form.

## 1.5 APPLICATION OF NANOTECHNOLOGY

The applications of nanotechnology, commonly incorporate industrial, medicinal, and energy uses and showed in Figure 1.7. These include more durable construction materials, therapeutic drug delivery, and higher density hydrogen fuel cells that are environmentally friendly. Nanoparticles and Nano devices are highly versatile through modification of their physiochemical properties, they have found uses in nanoscale electronics, cancer treatments, vaccines, hydrogen fuel cells, and Nano graphene batteries [20].



**Figure 1.7 Applications of nanotechnology**

### 1.5.1 Drug Delivery

One application of nanotechnology in medicine currently being developed involves employing nanoparticles to deliver drugs, heat, light or other substances to specific types of cells (such as cancer cells). Particles are engineered so that they are attracted to diseased cells, which allows direct treatment of those cells. This technique reduces damage to healthy cells in the body and allows for earlier detection of disease [21].

### **1.5.2 Diagnostic Techniques**

Researchers at Worcester Polytechnic Institute are using antibodies attached to carbon nanotubes in chips to detect cancer cells in the blood stream. The researchers believe this method could be used in simple lab tests that could provide early detection of cancer cells in the bloodstream.

A test for early detection of kidney damage is being developed. The method uses gold nanorods functionalized to attach to the type of protein generated by damaged kidneys. When protein accumulates on the nanorod the color of the nanorod shifts. The test is designed to be done quickly and inexpensively for early detection of a problem [22].

### **1.5.3 Antibacterial Treatments**

Researchers at the University of Houston are developing a technique to kill bacteria using gold nanoparticles and infrared light. This method may lead to improved cleaning of instruments in hospital settings.

Researchers at the University of Colorado Boulder are investigating the use of quantum dots to treat antibiotic resistant infections.

### **1.5.4 Sensing**

Nanotechnology-on-a-chip is one more dimension of lab-on-a-chip technology. Magnetic nanoparticles, bound to a suitable antibody, are used to label specific molecules, structures or microorganisms. In particular silica nanoparticles are inert from the photophysical point of view and might accumulate a large number of dye(s) within the nanoparticle shell. Gold nanoparticles tagged with short segments of DNA can be used for detection of genetic sequence in a sample. Multicolor optical coding for biological assays has been achieved by embedding different-sized quantum dots into polymeric microbeads. Nanopore technology for analysis of nucleic acids converts strings of nucleotides directly into electronic signatures. Sensor test chips containing thousands of nanowires, able to detect proteins and other biomarkers left behind by cancer cells, could enable the detection and diagnosis of cancer in the early stages from a few drops of a patient's blood. Nanotechnology is helping to advance

the use of arthroscopes, which are pencil-sized devices that are used in surgeries with lights and cameras so surgeons can do the surgeries with smaller incisions. The smaller the incisions the faster the healing time which is better for the patients. It is also helping to find a way to make an arthroscope smaller than a strand of hair [23,24].

### **1.5.5 Dye Sensitized Solar Cells (DSSCs)**

DSSCs are a type of photo-electrochemical cell that could be a viable alternative to traditional photovoltaic technology. They also appeal to researchers because of its simple production process, low cost, environmentally acceptable components, and transparency. Two fluorine-doped tin oxide (FTO) glass substrates make up the DSSC components. Semiconductors having a wide bandgap and good photochemical stability. As a working electrode or photoanode, they are utilized. Wide band gap semiconductors, on the other hand, do not capable of absorbing visible light. As a result, photosensitizers such as dye molecules are used. light absorption is sensitized with anode material. The redox electrolyte is the most often used electrolyte couple. The counter electrode or cathode is generally a platinum-coated FTO substrate [25].

#### **Components of DSSC**

DSSC consists of a mesoporous n-type semiconductor as an anode coated on to the FTO (Fluorine-doped Tin Oxide) glass substrate, a photosensitizer, redox couple electrolyte and a counter electrode. A brief description of the components of DSSC are as follows:

#### **Anode**

The photoanodes /working electrodes in DSSCs are made up of mesoporous n-type semiconductors sensitized with dye molecules. In DSSCs, the photoanode is very significant. The photoanode should have a large surface area and be capable of transferring excited electrons from the LUMO level of dye to the conduction band of the FTO substrate quickly. Michel Gratzel discovered DSSC in 1991 by using nanosized mesoporous  $\text{TiO}_2$  nanoparticles as a transparent electrode because it has a large interior surface area to absorb the dye. These advances in photoanodes may help

to slow down the recombination process. Furthermore, growing well-ordered nanostructures such as nanorods, nanotubes, and nanowires on titania or alumina substrates over FTO is a multistep, cost-effective procedure [26].

### **Photosensitizer / Dye**

The photosensitizer is important in the DSSC because it absorbs solar energy and participates in the excitation process. It should be able to absorb the maximum amount of solar light from visible to near infrared wavelengths and should not degrade quickly. Metal-complex sensitizers, metal-free organic sensitizers, and natural sensitizers are the three categories of sensitizers. N3, N719, black dye, Z907, C101, K77, and other ruthenium-based dyes are often employed as sensitizers. Metal-free, organic dyes have various advantages over metal-complex dyes, including easy availability, a cost-effective production technique, and high molar extinction coefficients. Metal-free organic sensitizers have a lower DSSC efficiency, and the difficult synthesis procedure is one of the primary issues. Natural colours such as betalains, carotenoids, anthocyanins, and chlorophyll pigments are derived from flowers, fruits, plants, leaves, and roots. Various natural dyes such as Bougainvillea, Golden trumpet, Bahraini henna, Cherries, Raspberries, Solanum Procumbens (SP), Solanum Torvum (ST), Artabotrys Hexapetalus (AH), Galinsoga Parviflora (GP) and Jasminum Grandiflorum L (JG) have been investigated with the photovoltaic performance of DSSCs [27].

### **Counter Electrode**

To complete the electrochemical cycle of the DSSC, an effective catalytic material is required for the rapid reduction of the oxidized component of the redox couple. Platinum and carbon-based materials are the most often employed catalysts in DSSCs. Platinum is distinguished by its low counter electrode resistance, which allows for a wide range of current and voltage. Platinum has the advantage of having exceptional catalytic activity, but it also has the disadvantage of being quite expensive. Carbon based counter electrode provides a cost-effective alternative for counter electrode manufacturing.

## **Electrolytes**

During the operation of the DSSC, electrolytes are responsible for electron transport between electrodes and dye regeneration. The dispersion of charge carriers in the electrolyte and the resistance owing to charge transfer at the electrolyte-electrode contact have a big impact on the FF [28]. An electrolyte must be strongly conductive while also allowing charge carriers to diffuse more quickly from the working electrode to the counter electrode. Better electrolytes should have excellent stability, including thermo-electrochemical, optical, and interfacial stability, and should not degrade dye molecules sensitized by the semiconducting material.

### **1.5.6 Nano particle fuel additives**

Nanomaterials can be used in a variety of ways to reduce energy consumption. Nanoparticle fuel additives can also be of great use in reducing carbon emissions and increasing the efficiency of combustion fuels. Cerium oxide nanoparticles have been shown to be very good at catalyzing the decomposition of unburnt hydrocarbons and other small particle emissions due to their high surface area to volume ratio, as well as lowering the pressure within the combustion chamber of engines to increase engine efficiency and curb NO<sub>x</sub> emissions [29]. Addition of carbon nanoparticles has also successfully increased burning rate and ignition delay in jet fuel. Iron nanoparticle additives to biodiesel and diesel fuels have also shown a decrease in fuel consumption and volumetric emissions of hydrocarbons by 3-6%, carbon monoxide by 6-12% and nitrogen oxides by 4-11% in one study.

### **1.5.7 Electronics**

Nanotechnology has helped break down barriers and bypass restrictions in the field of electronics. Nanoelectronics refers to the application of nanotechnology in electronic devices, especially transistors. Although the term nanotechnology means using technology less than 100 nanometers in size, nanoelectronics often refers to very small transistors, so quantum mechanical properties and inter-atomic interactions are required to be studied in-depth and extensively. Some nanoelectronic candidates include carbon nanotubes, silicon nanowires, hybrid molecular/semiconductor electronics or advanced molecular electronics. Nanoelectronics offers smaller faster,

and more portable systems [30]. It increases the capabilities of electronic devices, components, and integrated systems and enhances the density of memory chips to manage and store larger amounts of data and information. Nanoelectronics provides magnetic nanoparticles for data storage, printable and flexible electronics and advanced display technologies with quantum computing and conductive nanomaterials. They can improve display screens on electronic devices and revolutionize a lot of electronic products, applications, and procedures and reduce their weight, power consumption and the size of transistors used in integrated circuits [31].

### **1.5.8 Hydrogen Fuel Cells**

Nanotechnology is enabling the use of hydrogen energy at a much higher capacity. Hydrogen fuel cells, allow for storing energy from sunlight and other renewable sources in an environmentally-friendly fashion without any CO<sub>2</sub> emissions. Some of the main drawbacks of traditional hydrogen fuel cells are that they are expensive and not durable enough for commercial uses. However, by using nanoparticles, both the durability and price over time improve significantly. Furthermore, conventional fuel cells are too large to be stored in volume, but researchers have discovered that nanoblades can store greater volumes of hydrogen that can then be saved inside carbon nanotubes for long-term storage [32]

## **1.6 REVIEW OF LITERATURE**

Seong bum kim et.al., [33] have investigated the effect of graphene in dye sensitized solar cell prepared by using on nitrogen – doped Titanium oxide by sol gel method. The graphene in the photoelectrodes was confirmed by using TEM, XRD and Raman spectroscopy analysis. The maximum power conversion efficiency of Dye Sensitized solar cell for Graphene/Nitrogen doped titanium oxide Photo electrodes was reparsed as **9.32%**.

Guixiang Xie et.al., [34] have reported the application of doped rare earth oxide titanium oxide:(Tm<sup>3+</sup>, Yb<sup>3+</sup>) synthesized by hydrothermal method. The power conversion efficiency were confirmed by XRD,I-V Characteristic and XPS.A DSSC



containing  $Tm^{3+}/Yb^{3+}$ , achieves a conversion efficiency of **7.05%** which is increased by 10.0% compared with a DSSC lacking  $Tm^{3+}/Yb^{3+}$ .

Jing Li et al., [35] have reported the synthesis of transition metals into nitrogen-doped carbon as counter electrode catalyst for dye sensitized solar cell by using modified pyrolysis method as counter electrode materials in I-mediated dye sensitized solar cells. Ta/Co-N-C exhibits a superior catalytic and electrochemical stability than Co-N-C resulting in a high power conversion efficiency of **7.96%**.

Nitrogen doped porous carbon with well-balanced charge conduction and electrocatalytic activity for dye sensitized solar cells were synthesized by hard-template method [36]. Nan Xiao et al., synthesized the higher power conversion efficiency was confirmed by SEM, TEM, HRTEM and CV. The nitrogen doped porous carbon delivers higher power conversion efficiency **8.75%**

Enhanced photovoltaic performance of dye sensitized solar cell based on nickel oxide supported on nitrogen doped graphene nanocomposite as a photoanode were synthesized by Palraj Ranganathan [37]. XRD, FE-SEM, TEM, and FT-IR confirm the successful formation of the nanocomposite. The DSSCs based on Nitrogen Doped graphene oxide /NiO/TiO<sub>2</sub> nanocomposite based photo-anode exhibits a high power conversion efficiency of **9.75%**.

Sulfur doped reduced graphene oxide/MoS<sub>2</sub> composite with exposed active sites as efficient Pt-free counter electrode for dye sensitized solar cell were synthesized by Yanfang Wang [38]. The S doped rGO/MoS<sub>2</sub> composites were synthesized via a one-step annealing process at a moderate condition. The morphology of the sample was observed using a field emission scanning electron microscope. The sulfur doped reduced graphene oxide nanocomposite exhibits a high power conversion efficiency of **6.96%**.

Yi Di have reported the nitrogen and sulfur dual doped chitin derived carbon/graphene composites as effective metal free electrocatalysts for dye sensitized solar cells synthesized via modified hummers method and hydrothermal method [39]. The reduced graphene oxide/sulfur co-doped carbon composite achieved a higher power conversion efficiency of **6.36%**.

SnO<sub>2</sub>/ ZnO composite dye sensitized solar cells with graphene based counter electrodes were synthesized by K.Robinson. This Dye coted SnO<sub>2</sub>/ZnO composite film electrode were prepared by thin film coating method [40]. The best dye sensitized solar cells gives **5.5%** conversion efficiency.

Growth of aligned polypyrrole acicular nanorods and their application as Pt-free semitransparent counter electrode in dye sensitized solar cell were reported by Purushottam Jha. The PPy films were characterized by FTIR and UV- Visible spectroscopy [41]. The fabricated dye sensitized solar cell with N719 dye/TiO<sub>2</sub> as photoanode and PPy/FTO as counter electrode shows **1.7%** efficiency.

Natural hibiscus dye and synthetic organic eosin dye sensitized solar cells using titanium dioxide nanoparticles as photo anode: comparative study was reported by Swati S. Kulkarni. Titanium dioxide (TiO<sub>2</sub>) nanoparticles have been synthesized by the cost sol-gel technique [42]. The characteristics of TiO<sub>2</sub> nanoparticles were investigated by X-ray and Fourier Transform Infrared spectroscopy. Simple preparation method, wide availability, low cost and environmental friendliness of these dyes make them attractive for their use as sensitizers in dye sensitized solar cells.

Algal buffer layers for enhancing the efficiency of anthocyanins extracted from rose petals for natural dye sensitized solar cell were prepared by N. Prabavathy [43]. This paper lists the important factors they are responsible for anthocyanin instability in DSSC. TiO<sub>2</sub> nanorods prepared by hydrothermal method were used as photoelectrode and more characterized by XRD, TEM, and UV-Vis. The resulted DSSC with spirulina extract showed an enhanced efficiency of 1.47%.

Tungsten disulfide nanoparticles anchored on reduced graphene oxide for dye sensitized solar cell applications were synthesized by Sanjeev Kumar. The synthesized materials have been characterized for structural, compositional and optical properties by different techniques. Results showed that WS<sub>2</sub> nanoparticles were uniformly anchored on as well as in between the surface of rGO which helps to inflate the exfoliation of rGO stacked layers. Thus, the rGO/WS<sub>2</sub> hybrid can be used as counter electrode (CE) in dye sensitized solar cells. sheets which acted as nanospacers leading to exfoliation of rGO sheets and provided large active surface

area. The K of rGO/WS<sub>2</sub> hybrid was found to be 2.94%, close to Pt based reference CE [44].

## 1.7 CHARACTERIZATION TECHNIQUES

The crystallography, identification of organic, inorganic and polymeric materials, surface topography, compositional information, elemental analysis, atomic structure and detection of heavy metals of synthesized nanoparticles are determined by using different characterization techniques such as X-ray diffraction, Fourier Transform Infrared Microscopy, Field Emission Scanning Electron Microscopy, Energy Dispersive X-ray Spectroscopy and High Resolution Transmission Electron Microscopy

### 1.7.1 X-ray Diffraction (XRD)

The crystalline phases of the prepared nanocomposites are studied using XRD analysis. In a crystalline solid, the constituent particles like atoms, ions or molecules are arranged in a regular order. An interaction of a particular crystalline solid with X-rays helps in investigating its actual structure, orientation, composition, phases, internal lattice strain and particle size. Crystals are found to act as diffraction gratings for X-rays and this indicates that the constituent particles in the crystals are arranged in planes at close distances in repeated patterns. The phenomenon of diffraction of X-rays by crystals is studied by W.L. Bragg and his father W.H. Bragg in 1913. [45]

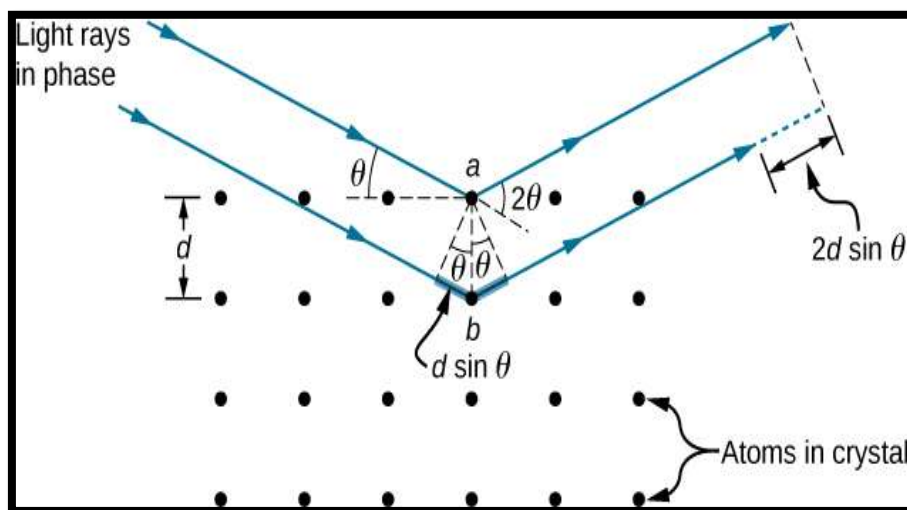


Figure 1.8 Schematic representation of X-ray diffraction

The X-ray diffraction patterns of the prepared nanocomposites are carried out using a X'PERT<sup>3</sup> Panalytical Diffractometer the finely powdered prepared nanocomposites are placed on the sample holder and X- Rays are directed towards the sample. The schematic representation of X-ray diffraction is showed in Figure 1.8. These X-Rays interacts with the atoms in the nanocomposites through constructive or destructive manner, when conditions satisfy Bragg's Law as depicted in Figure

$$n\lambda=2d \sin \theta$$

where,

$\lambda$  = wavelength of X-ray (Å),

$\theta$  = incident angle.

d = interlayer distance.

n = order of diffraction

The diffracted waves emitted by the array of atoms have the same frequency as that of incident rays. Thus the diffracted waves are then scanned, detected and recorded [46]

### **1.7.2 Field Emission Scanning Electron Microscopy (FESEM)**

The surface morphology of the prepared nanocomposites is characterized using Field Emission Scanning Electron Microscope (FESEM). It is a type of electron microscope that produces high-resolution images of the surface of the sample. FESEM equipped with diffracted backscattered electron detectors are used to examine the crystallographic orientation in materials. The FESEM images reveals about the morphology, structure and composition of the nanocomposites [47]. The surface of the sample can be clearly seen using three dimensional FESEM images

In this present work, ZEISS-SIGM field emission scanning electron microscopy is used for the analysis of surface morphology of prepared nanocomposites. ZEISS-SIGM field emission scanning electron microscopy is shown in the Figure 1.9. It is operated in the range of 30 keV and the areas are scanned in the range of 1 cm to 5 microns with its magnification ranging from 20 X to 30,000 X and its spatial resolution of about 50 to 100 nm. The electron beam from the tungsten

filament is directed towards the sample with an accelerating voltage of about 1 to 30 kV. This electron beam gets diverged and passes through a pair of electro-magnetic lenses and interacts with the sample and thus the interaction of electron beam with the sample results in the exhibition of secondary electrons, backscattered electrons and various energies of characteristic X-rays. The secondary electrons and the backscattered electrons are scanned and detected to investigate the surface morphology, crystallography and composition of the sample [48].



**Figure 1.9 ZEISS-SIGM Field Emission Scanning Electron Microscopy**

### **1.7.3 Fourier Transform Infrared Spectroscopy (FT-IR)**

Fourier Transform Infrared Spectroscopy (FT-IR) is used to investigate the molecular structures and bonding interactions of the prepared nanocomposites. The functional groups can be identified by measuring the spectrum of absorbed radiation.

The Infrared spectra are recorded using a Shimadzu IR affinity-1 spectrometer shown in the figure 1.10. FT- IR spectroscopic analysis is recorded in the range from far infrared region ( $400\text{ cm}^{-1}$ ) to the mid infrared region ( $4000\text{ cm}^{-1}$ ). This spectrometer uses infrared light and the spectrum depicts the transmission and absorbance of light for all the infrared wavelengths [49]. When the sample is irradiated by a broad spectrum of infra-red light, it absorbs the radiation and the chemical bonds tend to vibrate at characteristic frequencies. The radiation absorbed at

particular frequency produces a spectrum that can be used to determine the functional groups and compounds, since the chemical bonds absorb infrared energy at specific frequencies. The plot of the IR transmission versus frequency is its "fingerprint" which can be compared to reference spectra to classify the material [50]



**Figure 1.10 Shimadzu IR affinity-1spectrometer**

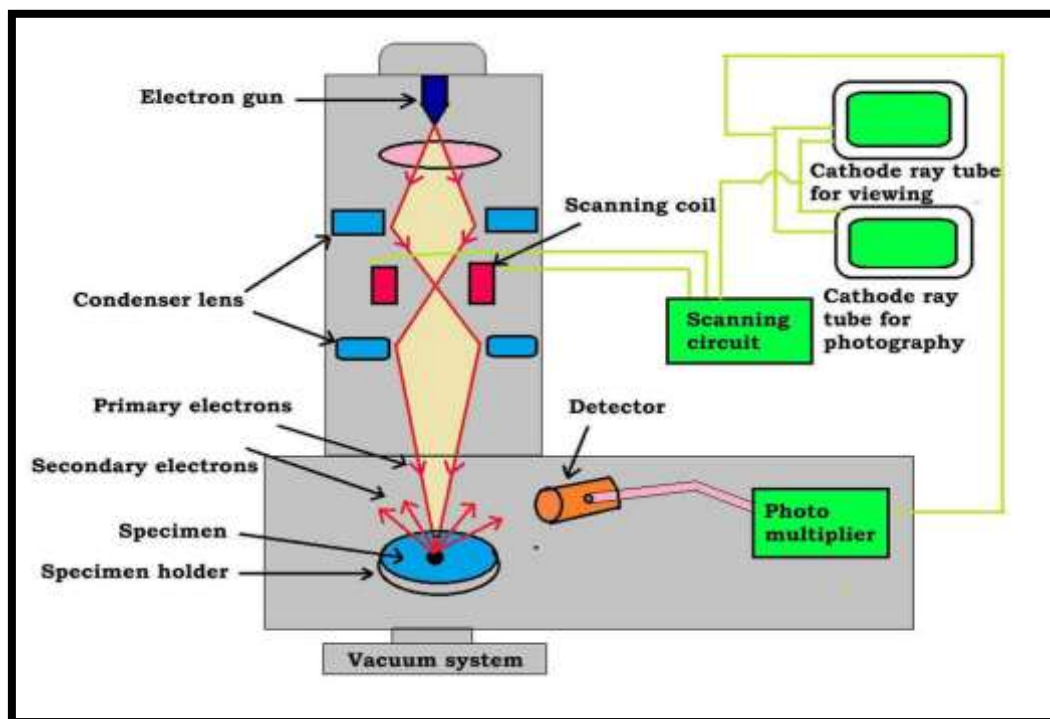
#### **1.7.4 Energy Dispersive X-ray Analysis (EDAX)**

Energy dispersive X-ray spectrometers take advantage of the photon nature of light. In the X-ray range the energy of a single photon is just adequate to produce a measurable voltage pulse at the output of an ultra-low noise preamplifier connected to the semiconductor detector crystal. The individual pulse heights are a statistical measure related to quantum energy. By recording and counting a great number of such pulses within a so-called multichannel analyzer, a complete image of the X-ray spectrum is built up almost simultaneously. This digital quantum counting technique makes the energy dispersive spectrometry extremely consistent[51].

#### **1.7.5 High-resolution transmission electron microscopy (HRTEM)**

High Transmission Electron Microscopy (HRTEM) is extensively used for measuring the particle size of nanoparticles. The principle of operation of TEM is same as that of the optical microscope, but in this case a beam of electrons is used instead of light.

In this present work, Jeol JEM 210 is used to generate higher resolution transmission electron microscope images. When monochromatic electron beam strikes the sample, some of the electrons are scattered and some are transmitted. The transmitted electrons are then passed through an objective lens which gives an inverted image. An objective aperture is placed at the back of the objective lens to form an image [52]. The first image generated by the objective lens is further projected onto a phosphorus coated screen which emits visible light. The brighter areas of the image indicate the passage of more number of electrons whereas the darker areas represent that only few electrons have passed through it. Some other effect produced by striking electron is that it emits X-ray photons, Auger electrons, secondary electrons, backscattered electron, etc. Many of these effects are used for characterizing the specimen as shown in the Figure 1.11. Thus TEM record the information carried by transmitted electrons, scattered as well as elastically and in elastically scattered electrons [53].



**Figure 1.11 Schematic representation of HR- TEM**

### 1.7.6 Raman Spectroscopy

In all three states of matter, Raman spectroscopy can be used. This approach is non-destructive, unambiguous, and does not necessitate sample preparation. In this present work Tech 1 (QEB0120) model Raman Spectroscopy is used [54].

A substance is irradiated with monochromatic light in Raman spectroscopy, and the scattered light is detected by a spectrometer. By absorption and scattering, photons from the light source interact with the molecules in the sample. The type of light scattering might be elastic or inelastic. Scattering is an elastic scattering phenomenon, while Raman scattering is an inelastic scattering mechanism. The dispersed photon's electric component attracts electrons in the molecule, causing it to be stimulated to a virtual state. When an excited electron relaxes to vibrational energy levels that are either greater or lower than the starting level, Raman scattering occurs [55].

### 1.7.7 Solar simulator

A Xenon light source is used in the solar simulator. 50 reflectors and air mass filters are used to meet the basic parameters of the light source in compliance with international requirements for using Xenon light as a solar simulator. Solar simulators are classed into three classes by international standards: Class A, Class B, and Class C. A solar simulator should have a good spectral match to sunshine, a consistent light source, and long-term stability. This electrochemical workstation can be tailored to suit any application in the field of traditional electrochemistry. Current- Voltage and EIS analysis capable module and a low current option can be added to the SP-150 potentials and showed in Figure 1.12 and 1.13 [56].



**Figure 1.12 SP 150 Biologic Instrument**





**Figure 1.13 Light Source for Solar simulator**

### **1.7.8 UV-Visible spectroscopy**

Absorption of electromagnetic radiation in the ultraviolet to infrared range causes bound or free electrons to make transition to less or more stable anti-bonding orbitals. When a light source illuminates an unknown prepared sample, the atoms in the unknown sample absorb certain wavelengths in the UV to IR areas [57]. The samples can be analysed qualitatively and quantitatively using UV-Visible spectroscopy. The UV-Vis absorption spectra are measured in the diffuse reflectance mode with a Cary 60 UV-Vis model spectro-photometer shown in the Figure 1.14, and the spectral range of 200 to 800 nm with a resolution of 2 nm in the current investigation.



**Figure 1.14 Cary 60 UV-Vis Spectrometer**

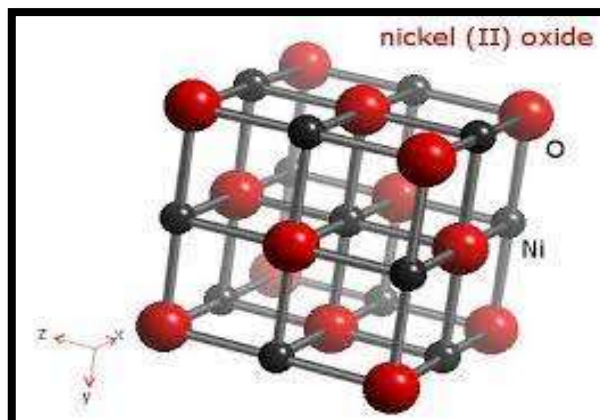
## **1.8 Materials**

### **1.8.1 Nickel Oxide (NiO)**

Nickel (II) oxide is the chemical compound with the formula NiO and showed in Figure 1.15. It is the principal oxide of nickel. It is classified as a basic metal oxide. Several million kilograms are produced annually of varying quality, mainly as an intermediate in the production of nickel alloys. The mineralogical form of NiO, bunsenite, is very rare. Other nickel(III) oxides have been claimed, for example: Ni<sub>2</sub>O<sub>3</sub> and NiO<sub>2</sub>, but they have yet to be proven by X-ray crystallography [58].

NiO has a partially filled 3d-band (the Ni atom has 8 of 10 possible 3d-electrons) and therefore would be expected to be a good conductor [59]. However, strong Coulomb repulsion (a correlation effect) between d-electrons makes NiO instead a wide band gap Mott insulator. Thus, strongly correlated materials have electronic structures that are neither simply free-electron-like nor completely ionic, but a mixture of both.

### **Crystal structure**



**Figure 1.15 Crystal structure of Nickel oxide**

NiO adopts the NaCl structure, with octahedral  $\text{Ni}^{2+}$  and  $\text{O}^{2-}$  sites. The conceptually simple structure is commonly known as the rock salt structure. Like many other binary metal oxides, NiO is often non-stoichiometric, meaning that the NiO ratio deviates from 1:1. In nickel oxide, this non-stoichiometry is accompanied by a color change, with the stoichiometrically correct NiO being green and the non-stoichiometric NiO being black [60].

### 1.8.2 YITTRIUM OXIDE ( $\text{Y}_2\text{O}_3$ )

Yttrium oxide ( $\text{Y}_2\text{O}_3$ ) nanoparticle is an air-stable, solid substance white in color. It is used in the field of material sciences, to make phosphors that are used in imparting the red color of the picture tubes in televisions. Another major use of the yttrium oxide nanoparticles is in inorganic synthesis. Yttrium belongs to Block D, Period 5 and oxygen belongs to the Block P, Period 2 in the periodic table [61].

#### Chemical properties

- Chemical symbol -  $\text{Y}_2\text{O}_3$
- Group – Yttrium 3
- Oxygen 16
- Electronic Configuration – Yttrium  $\text{Kr } 4d^1 5s^2$   
Oxygen  $1s^2 2s^2 2p^4$

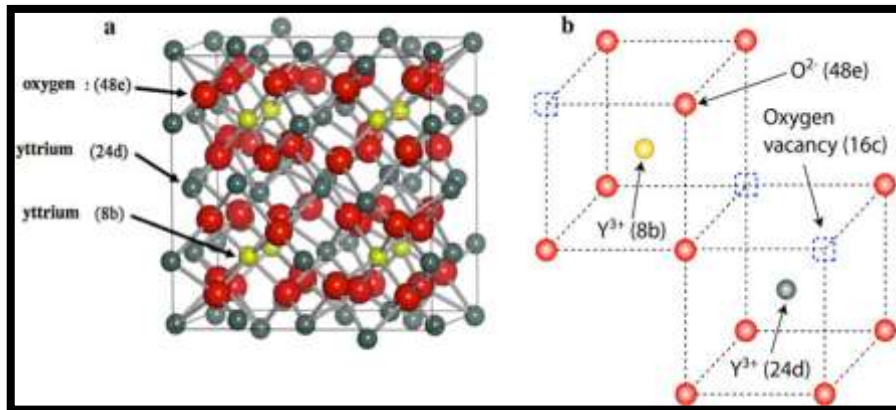
#### Chemical composition

- Yttrium – 78.77%
- Oxygen – 21.1%

#### Physical Properties

- Density - 5.01 g/mL
- Molecular Weight – 225.81

## Crystal Structure



**Figure 1.16 Crystal structure of Yttrium oxide**

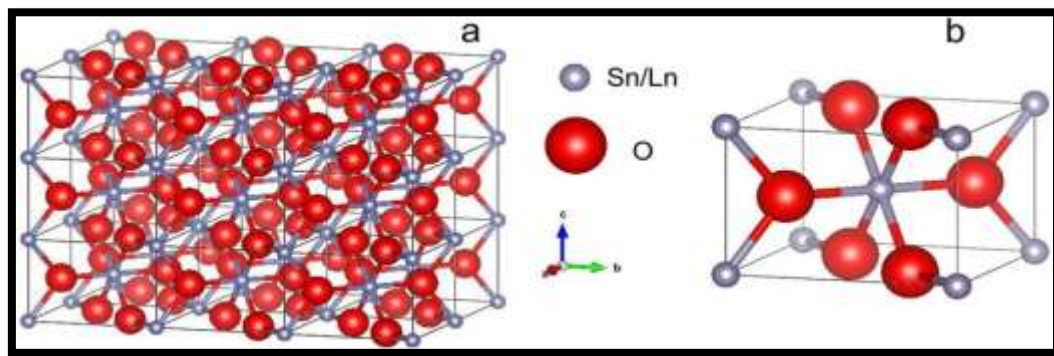
Yttrium (yttria) is a body-centered cubic material with bixbyite or cubic-C structure. Yttrium ions occupy two different sites: eight octahedral sites with  $C_{3i}$  point symmetry and 24 prismatic sites with  $C_2$  symmetry and the crystal structure of Yttrium oxide is showed in Figure 1.16. Six oxygen ions surround each yttrium ion [62]. Ion positions in the unit cell are known from both X-ray and neutron-diffraction measurements. Optical-quality, single-crystal yttria is typically made by the flame-fusion technique, and optical-quality sintered polycrystalline yttria is available in a variety of window shapes. Yttria is an excellent trivalent-ion host material for solid-state lasers. A variety of candidate metal-ion dopants and many other rare earth metals have been investigated. Yttria has a band gap of approximately 6.0 eV [63].

### 1.8.3 Tin Oxide ( $\text{SnO}_2$ )

Tin oxide ( $\text{SnO}_2$ ) is also known as stannic oxide. It can be found naturally as the mineral cassiterite. It is typically a white to off-white and sometime grey crystalline solid. The electronic band gap of  $\text{SnO}_2$ , known to be n-type, is about 3.5 eV. Because of the outstanding electrical, optical, and electrochemical properties, tin oxide offers a wide range of applications in solar cells, catalytic support materials, transparent electrodes, and solid-state chemical sensors. Tin oxide is of technological interest for solid state gas sensors, transparent conducting electrodes, front electrodes of solar cell, and catalyst supports due to its chemical and mechanical stability [64].  $\text{SnO}_2$  is used as a transparent conductor due to its stability,

low electrical resistivity and high optical transparency in the visible region. Bulk SnO<sub>2</sub> is known to behave as a direct band gap semiconductor with selection rules due to their special wave function symmetry making transitions forbidden, nanostructure materials are known to break this selection rule.

### Crystal Structure



**Figure 1.17 Crystal structure of Tin oxide**

Black,  $\alpha$ -SnO adopts the tetragonal PbO layer structure containing four coordinate square pyramidal tin atoms. This form is found in nature as the rare mineral romarchite. The asymmetry is usually simply ascribed to a sterically active lone pair however, electron density calculations show that the asymmetry is caused by an antibonding interaction of the Sn(5s) and the O(2p) orbitals and showed in Figure 1.17. The electronic structure and chemistry of the lone pair determines most of the properties of the material. Non-stoichiometry has been observed in SnO<sub>2</sub>. The electronic band gap has been measured between 2.5eV and 3eV.

#### 1.8.4 Solanum Procumbens (SP)

Solanum Hainanense is a synonym for Solanum Procumbens (SP) are showed in Figure 1.18. This is a rare medicinal plant with a limited distribution. Solanum is a large flowering plant species that comprises three commercially important food crops: potato, tomato, and eggplant (aubergine, brinjal). Polyphenols, terpenoids, steroids, alkaloids, and anthocyanin are among the numerous chemicals found in SP [65]. The major leaf pigment, chlorophyll, is produced during the light reaction of photosynthesis. In the reduction process of photosynthesis, an electron is converted from water to carbon dioxide. Chlorophyll plays an important role in this process by absorbing the energy of the sun.



**Figure 1.18 Solanum Procumbens (SP)**

### **1.8.5 Solanum Torvum (ST)**

Solanum Torvum (ST) is a prickly tomentose erect shrub leaves having no prickles white ball shaped flowers and lobed fruits sealed on the calyx belonging to the family solanaceae which is showed in Figure 1.19. Solanum Torvum (ST)) family is known for possessing a wide range of therapeutic properties, this extract contains a high amount of phytochemical properties Leaves have been reported to contain the triaconlanol, sterols, terpenoids, campestero and anthocyanin [66]. The sapogenin steroid chlorogenin is another of the potentially active compounds found in turkey berries which can help to increase the photosynthesis process.



**Figure 1.19 Solanum Torvum (ST)**

### **1.8.6 Artabotrys Hexapetalus (AH)**

Artabotrys Hexapetalus (AH) is distributed throughout the southern part of in India. As a Indian traditional folk medicine and showed in Figure 1.20. Its roots and

fruits are used for treating malaria and scrofula respectively. *Artabotrys hexapetalus* is a medicinal plant that's also known in India by the common name "Manorangini." AH extract are belonging to the Annonaceae family and this chlorophyll extract are not degrading for long time [67]. AH extract contains rich polyphenols that helps for the photosynthesis process and hence this can be a more efficient absorber of DSSC.



**Figure 1.20 Artabotrys Hexapetalus (AH)**

### **1.8.7 Galinsoga Parviflora (GP)**

*Galinsoga parviflora* is an Asteraceae family herbaceous plant. Guasca, mielcilla, piojito, galinsoga, gallant soldier, quick weed, and potato weed are some of its common names. *Galinsoga Parviflora* (GP) is a common plant which extracts are high in electron-rich polyphenols, amino acids, anthocyanin and chlorogenic acid and showed in Figure 1.21 Hence chlorogenic acid is a good chemical sensitizer found in GP dye, hence this extract may function as a good DSSC sensitizer [68].



**Figure 1.21 Galinsoga Parviflora (GP)**

### 1.8.8 Jasminum Grandiflorum L (JG)

Benzyl acetate (23.7%), benzyl benzoate (20.7%), phytol (10.9%), linalool (8.2%), isophytol (5.5%), geranyl linalool (3.0%), methyl linoleate (2.8%), and eugenol are the main constituents of *J. grandiflorum* (2.5%). The renowned jasmine fragrance is made up of these ingredients. The molecular structure of the jasmonate plant hormones was extracted from the jasmine oil *Jasminum Grandiflorum* and showed in Figure 1.22. The leaves of *Jasminum Grandiflorum L (JG)* are used in the treatment of fixing loose teeth and skin disease. The extract from JG contain high level chlorophyll which are useful for DSSCs [69].



**Figure 1.22 of *Jasminum Grandiflorum L (JG)***

### 1.9 Scope of the Work

Recently, graphene oxide based nanocomposites have been receiving considerable attention as a result of their unique properties that leads to tremendous applications in various fields like optics, Supercapacitor, electronics, biomedicine, magnetic, mechanics, catalysis and energy science. Further, on compositing it with, metal oxides, semiconductor etc., will improve their existing properties. Hence, the main scope of the present work is

- Synthesis of Graphene oxide by Modified Hummers method
- Embellishment of various concentration of metal oxides (Nickel oxide, Yttrium oxide and Tin oxide) on Graphene oxide nanosheet.



- Preparation of Natureal Dyes (SP, ST, AH, GP and JG) for DSSCs
- To characterize the nanocomposites for optical, structural and morphological studies HR-TEM, FT-IR, XRD and FESEM respectively.
- Investigation of photo-current of prepared counter electrode

### 1.9.1 Methodology

The methodology used to accomplish the objectives is shown in the Figure 1.23

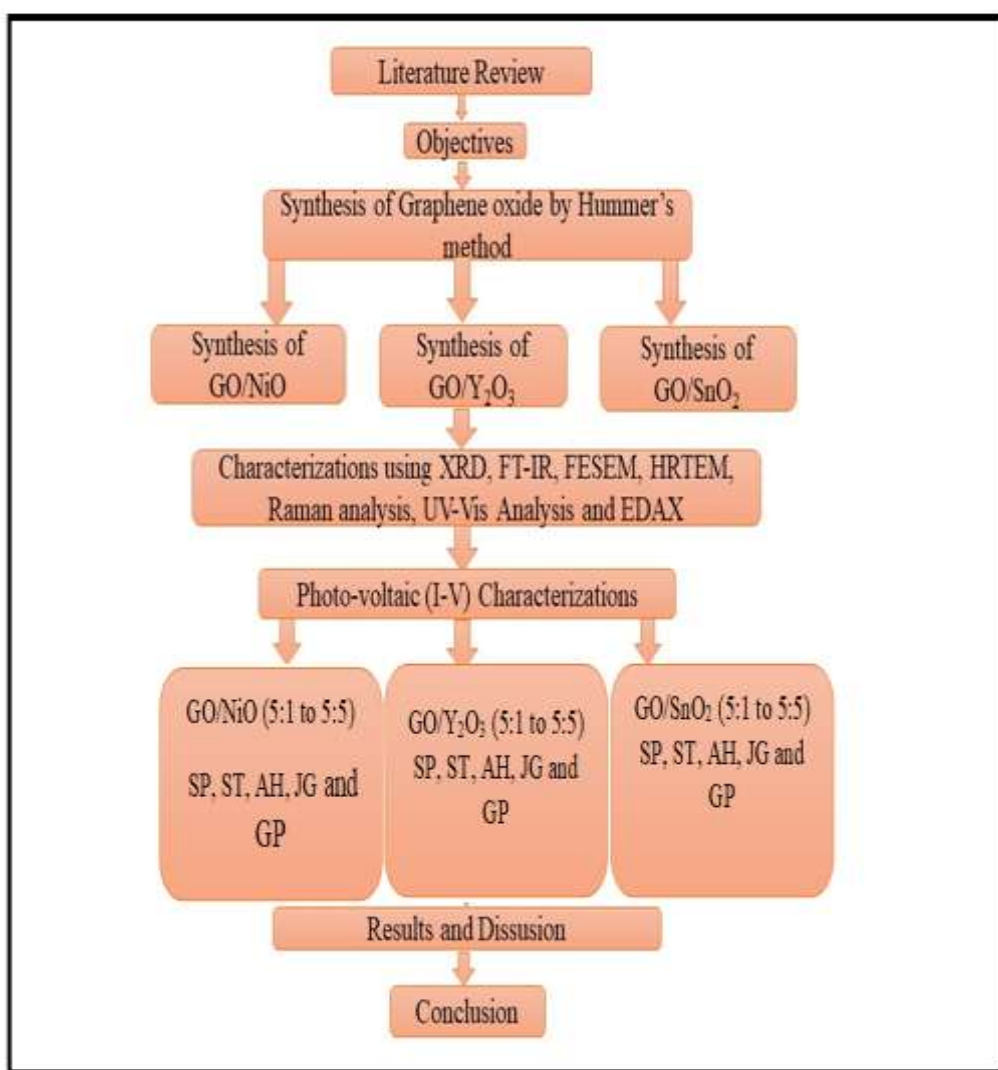


Figure 1.23 Methodology

## 1.9.2 Organization of Thesis

**CHAPTER-I** describes the significance of Nanoscience and Nanotechnology and its vital role in various fields. It deals with the introduction and properties of Graphene oxide, Nickel oxide, Yttrium oxide and Tin oxide for various applications and also discuss the various natural dyes as a sensitizer in DSSCs. It discusses the detailed review of relevant literature which opens up the way for the various applications. It also outlines the instruments used for the characterization of synthesized nanomaterials.

**CHAPTER-II** deals about the synthesis of Graphene oxide by modified hummer's method in which graphite is treated with a mixture of very strong oxidizers such as sodium nitrate, sulphuric acid and potassium permanganate. The crystalline structural, morphological and functional properties of the nanocomposites are investigated by X-Ray diffraction (XRD), Field Scanning Electron Microscopy (FSEM), energy dispersive X-ray (EDAX), High resolution transmission electron microscopy (HR-TEM) and Fourier Transform spectroscopy (FT-IR). The UV-Vis absorption study and Raman spectra are recorded.

**CHAPTER-III** describes the influence of different concentrations (5:1, 5:2, 5:3, 5:4 and 5:5) of Nickel oxide nanoparticles blended on the surface of GO nanosheet. The high crystalline diffraction peaks of Nickel oxide nanoparticles are in well agreement with the JCPDS card no (47-1049). FESEM analysis also confirmed that the NiO nanoparticles are equally merged on the surface of GO nanosheet.

**CHAPTER-IV** explains the synthesis of various concentrations (5:1, 5:2, 5:3, 5:4 and 5:5) of Yttrium oxide ( $Y_2O_3$ ) nanoparticles on the surface of GO nanosheet. Structural, morphological, and elemental composition of synthesized nanocomposites by FT-IR, XRD, FESEM, EDAX techniques confirmed that the  $Y_2O_3$  nanoparticles are equally blended on the surface of GO nanosheet.

**CHAPTER-V** describes the synthesis of various concentrations of  $SnO_2$  nanoparticles are blended graphene oxide nanosheet. The structural, morphological and functional properties of the prepared nanocomposites are examined. The influence of various concentrations of the  $SnO_2$  nanoparticles (5:1, 5:2, 5:3, 5:4 and

5:5) on the Graphene Oxide nano sheet is analysed. The diffraction peaks of SnO<sub>2</sub> nanoparticles from XRD analysis are in well accordance with the SAED pattern of HRTEM.

**CHAPTER-VI** describes the investigation of Efficiency studies for GO/NiO (5:1, 5:2, 5:3, 5:4 and 5:5) as a counter electrode and Solanum Procumbens (SP), Solanum Torvum (ST), Artabotrys Hexapetalus (AH), Galinsoga Parviflora (GP) and Jasminum Grandiflorum L (JG) and natural extracts as a sensitizer for Dye sensitized solar cell application.

**CHAPTER-VII** describes the investigation of Efficiency studies for GO/Y<sub>2</sub>O<sub>3</sub> (5:1, 5:2, 5:3, 5:4 and 5:5) as a counter electrode and Solanum Procumbens (SP), Solanum Torvum (ST), Artabotrys Hexapetalus (AH), Galinsoga Parviflora (GP) and Jasminum Grandiflorum L (JG) as a sensitizer for Dye sensitized solar cell application.

**CHAPTER VIII** describes the investigation of Efficiency studies for GO/SnO<sub>2</sub> (5:1, 5:2, 5:3, 5:4 and 5:5) as a counter electrode Solanum Procumbens (SP), Solanum Torvum (ST), Artabotrys Hexapetalus (AH), Galinsoga Parviflora (GP) and Jasminum Grandiflorum L (JG) natural extract as a sensitizer for Dye sensitized solar cell application.

**CHAPTER-XI** Summary and Conclusion of the results and scope of the future research work.

## REFERENCES

1. S. Logothetidis, Nanostructured Materials and Their Applications, NanoScience and Technology, DOI 10.1007/978-3-642-22227-6 1,(2012)
2. K. Eric. Drexler, Anchor Books and Doubleday, Engines of Creation :The Coming Era of Nanotechnology,(1986).
3. B. Bhushan, Springer Handbook of Nanotechnology, DOI 10.1007/978-3- 319-49347-3\_1,(2017)
4. Guozhong Cao, Nanostructures and Nanomaterials, Synthesis, Properties, and Applications,(2008)
5. Alain Nouailhat, ISBN:978-1-84821-007-3
6. Physical Fundamentals of Nanomaterials, Elsevier, DOI: <https://doi.org/10.1016/B978-0-12-410417-4.00008-3>,(2018).
7. [www.safenano.org](http://www.safenano.org)
8. Satoshi Horikoshi and Nick Serpone, Introduction to Nanoparticles, (2013).
9. Jitendra N. Tiwari a, Rajanish N. Tiwari, Kwang S. Kim, Zero-dimensional, one-dimensional, two-dimensional and three-dimensional nanostructured materials for advanced electrochemical energy devices, Progress in Materials Science 57,724–803,(2012).
10. Jaison Jeevanandam , Ahmed Barhoum, Yen S. Chan, Alain Dufresne and Michael K. Danquah, Review on nanoparticles and nanostructured materials: history, sources, toxicity and regulations, Beilstein J. Nanotechnol, 9, 1050–1074,(2018).
11. Hassan Hassanien Mohamed Darweesh, Nanomaterials: Classification and Properties-Part I, Nanoscience, 1-11,(2017).
12. Dolez, P. I., Nanomaterials Definitions, Classifications, and Applications. Nanoengineering, 3–40, doi:10.1016/b978-0-444-62747-6.00001-4,(2015).

13. Sengupta, A and Sarkar, C. K, Introduction to Nano. Engineering Materials. doi:10.1007/978-3-662-47314-6,(2015)
14. Sandhiya sanand, Nanostructured materials; classification and methods of characterization, (2017).
15. www.doccity.com
16. Parvez Iqbal, Jon A. Preece and PaulaM. Mendes, Nanotechnology: The–Top-Down and –Bottom-Up Approaches, DOI: 10.1002/9780470661345.smc 195, (2012)
17. Andres La Rosa, Mingdi Yan, Rodolfo Fernandez, Xiaohua Wang and Elia Zegarra, Top-down and Bottom-up approaches tonanotechnology
18. Dr. V.M.Aroleand Prof.S.V.Munde, Fabrication of nanomaterials by top-down andbottom-upapproaches–anoverview,vol.1,issue2,page89-93,(2014).
19. Gritsch L., Meng D and Boccaccini A. R, Nanostructured biocomposites for tissue engineering scaffolds. Biomedical Composites, 501–542, doi:10.1016/b978-0-08-100752-5.00021-4,(2017).
20. www.britannica.com
21. Salim Barbhuiya and i Curtin Uni, Applications of Nanotechnology in Cement and Concrete Science, DOI: 10.4018/978-1-4666-6363-3.ch029, (2014).
22. A S Edelstein and R C Cammarata, Nanomaterials: Synthesis, Properties and Applications
23. www.news-medical.net
24. Karak, N, Fundamentals of Nanomaterials and Polymer Nanocomposites. Nanomaterials and Polymer Nanocomposites, 1–45. doi:10.1016/b978-0-12-814615-6.00001-1, (2019). Op andelec
25. <https://copublications.greenfacts.org/en/nanotechnologies/1-2/3-nanoparticle-properties.htm>

26. Hong, N. H, Introduction to Nanomaterials: Basic Properties, Synthesis, and Characterization. *Nano-Sized Multifunctional Materials*,1–19, doi:10.1016/b978-0-12-813934-9.00001-3, (2019).
27. [www.shellzero.wordpress.com](http://www.shellzero.wordpress.com)
28. Dan Guo, Guoxin Xie and Jianbin Luo, J, Mechanical properties of nanoparticles: basics and applications, *Phys. D: Appl. Phys.* 47, 013001, (2014)
29. Reghunadhan, A., Kalarikkal, N and Thomas, S, Mechanical Property Analysis of Nanomaterials. *Characterization of Nanomaterials*,191–212, doi:10.1016/b978-0-08-101973-3.00007-9, (2018)
30. Taufeeque Hasan, Mechanical Properties of Nanomaterials: A Review, Vol-2 Issue-4 *IJARIE-ISSN(O)-2395-4396* ,(2016)
31. Sandhya P K, Jiya Jose, M S Sreekala, M Padmanabhana, Nandakumar Kalarikkal , Sabu Thomas, 2018, Reduced graphene oxide and ZnO decorated graphene for biomedical applications, *Ceramics International* , <https://doi.org/10.1016/j.ceramint.2018.05.143>.
32. Yan-Wen Wang, Aoneng Cao, Yu Jiang, Xin Zhang, Jia-Hui Liu, Yuanfang Liu, and Haifang Wang, Superior Antibacterial Activity of Zinc Oxide/Graphene Oxide Composites Originating from High Zinc Concentration Localized around Bacteria, doi:10.1021/am4053317.
33. Seong-Bum, Kim Jun-Yong, Park Chan-Soo Kim, Kikuo Okuyama, Sung-Eun Lee, Hee-Dong Jang and Tae-Oh Kim. *ACP* <https://doi.org/10.1021/acs.jpcc.5b02309> 2015 **119**, 26 , 16552-16559
34. Guixiang, Xie, Yuelin, Wei; Leqing, Fan and Wu Jihuai, 2013 10.1088/1742-6596/339/1/012010
35. Jing Li, sining Yun, Xiao Zhou and Yuzhi Hou 2017, <http://dx.doi.org/10.1016/j.carbon.2017.10.010>
36. Nan Xiao, Junwei Song, Yuwei Wang, Chang Liu, Ying Zhou and Zhiqiang Liu *carbon* **128** 2018 201-204

37. Palraj Ranganathan, Ragu Sasikumar, Shen-Ming Chen, Syang-PengRwei and PedaballiSireesha <https://doi.org/10.1016/j.jcis.2017.06.012> **504**, 570-578
38. Yanfang Wang, Yanjun Guo, Wentao Chen, Qing Luo, Wenli Lu, Peng Xu, Dongliang Chen, Xiong Yin and Meng He <https://doi.org/10.1016/j.apsusc.2018.04.276> 2018, **452**, 232-238
39. YiDi, Zhanhai Xiao, Xiaoshuang Yan, Geying Ru, Bing Chen and Jiwen Feng *Applied Surface Science* 2018 **441**, 807-815
40. K.Robinson, G.R.A.Kumara, R.J.G.L.R.Kumara, E.N.Jayaweera and R.M.G.Rajapakse <https://doi.org/10.1016/j.orgel.2018.01.040>, 2018 **56**, 159-162
41. Purushottam Jha,P, Veerender,S.P, Koiry,C, Sridevi,A.K, Chauhan,K.P and Muthe,S.C. Gadkari **29** 2018, 401-406
42. Swati S. Kulkarni, S. S. Hussaini Gajanan A And Bodkhemahendra D. Shirsat <https://doi.org/10.1142/S0218625X18501640> **26** 2019
43. N. Prabavathy,S. Shalini,R. Balasundaraprabhu, Dhayalan Velauthapillai,S. Prasanna,G. Balaji,N. Muthukumarasamy **42** 2018 790-801
44. Sanjeev Kumar, Om Prakash, Aman Mahajan and Vibha Saxena <https://doi.org/10.1063/1.5028732>, 2018
45. Chandrama Sarkar and Swapan K. Dolui, Synthesis of copper oxide/reduced graphene oxide nanocomposite and its enhanced catalytic activity towards reduction of 4-nitrophenol, *RSC Adv*, 5, 60763–60769,(2015)
46. Kangfu Zhou, Yihua Zhu, Xiaoling Yanga, Jie Luo, Chunzhong Li and Shaorong Luan, A novel hydrogen peroxide biosensor based on Au– graphene–HRP–chitosan biocomposites, *Electrochimica Acta*,(2010).
47. Ajay Gupta, Ramen Jamatia, Ranjit A. Patil, Yuan-Ron Ma and Amarta Kumar Pal, Copper Oxide/Reduced Graphene Oxide Nanocomposite- Catalyzed Synthesis of Flavanones and Flavanones with Triazole Hybrid Molecules in One Pot: A Green and Sustainable Approach, *ACS Omega*, 3, 7288–7299,(2018).

48. J.Vinoth Kumar, R.Karthik, Shen-Ming Chen, K.Saravanakumar, Govindasamy Mani, V.Muthuraj, Novel hydrothermal synthesis of MoS<sub>2</sub> nanoclusters structure for sensitive electrochemical detection of human and environmental hazardous pollutant 4-aminophenol, RSC Advances, DOI: 10.1039/C6RA03343A,(2016).
49. Manish Kumar, Unni Krishnan, Pooja Devi and Akshay Kumar, Structural analysis of graphene oxide/silver nanocomposites optical properties, electrochemical sensing and photocatalytic activity, J Mater Sci: Mater Electron, DOI 10.1007/s10854-017-7881-7, (2017).
50. Tamas Nemeth, Peter Jankovics, Julia Nemeth-Palotas, Hilda Kocsis, Szeged-Szalai, Determination of paracetamol and its main impurity 4-aminophenol in analgesic preparations by micellar electrokinetic chromatography, Journal of Pharmaceutical and Biomedical Analysis, 47, 746–749,(2008).
51. Graziella Scandurra, Arena Antonella, Carmine Ciofi, Gaetano Saitta and Maurizio Lanza, Electrochemical Detection of p-Aminophenol by Flexible Devices Based on Multi-Wall Carbon Nanotubes Dispersed in Electrochemically Modified Nafion, Sensors, 14, 8926-8939; doi:10.3390/s140508926,(2014).
52. Priya Arulselvi Ramasubramanian, Sakthivel Thangavel, Gouthami Nallamuthu., Kiranpreethi Kirabakaran, Vinesh Vasudevan, Kennedy Ravichandran and Gunasekaran Venugopal, Journal of Materials Science: Materials in Electronics. <https://doi.org/10.1007/s10854-018-8539-9>,(2017).
53. Leandro Yoshio Shiroma, Murilo Santhiago, Angelo L. Gobbi, Lauro T. Kubota, Separation and electrochemical detection of paracetamol and 4-aminophenol in a paper-based microfluidic device, Electrochimica Acta, vol.194, pg.no:116–126,(2016).
54. Huanshun Yin, Qiang Ma, Yunlei Zhou, Shiyun Ai and Lusheng Zhu, Electrochemical behavior and voltammetric determination of 4-aminophenol based on graphene–chitosan composite film modified glassy carbon electrode, Electrochimica Acta 55,7,102–110,(2010).



55. A.T.Ezhil Vilian, Vedyappan Veeramani, Shen-Ming Chen, Rajesh Madhu, Yun, Suk and Huh, Young-Kyu Han c, Preparation of a reduced graphene oxide/poly-lglutathione nanocomposite for electrochemical detection of 4- aminophenol in orange juice samples, *Analytical methods*, 00, 1-3,(2013).
56. Anna Regiel-Futyra, Ma gorzata Kus-Li kiewicz, Victor Sebastian, Silvia Irusta, Manuel Arruebo, Grazyna Stochel, and Agnieszka Kyzio, Development of non-cytotoxic chitosan-gold nanocomposites as efficient antibacterial materials, *ACS Applied Materials & Interfaces*, DOI: 10.1021/am508094e, (2014)
57. S. Govindan, E. A. K. Nivethaa, R. Saravanan, V. Narayanan and A. Stephen, (2012), Synthesis and characterization of chitosan–silver nanocomposite, *Appl Nanosci*2:299–303.
58. Richard Justin and Biqiong Chen, Strong and conductive chitosan–reduced graphene oxide nanocomposites for transdermal drug delivery, *J. Mater. Chem. B*, 2, 3759–3770,(2014)
59. Dasan Mary Jaya Seema, Bullo Saifullah, Mariadoss Selvanayagam, Sivapragasam Gothai, Mohd Zobir Hussein, Suresh Kumar Subbiah, Norhaizan Mohd Esa and Palanisamy Arulselvan, Designing of the Anticancer Nanocomposite with Sustained Release Properties by Using Graphene Oxide Nanocarrier with PhenethylIsothiocyanate
60. Yang L, Carbon nanostructures, *Nanotechnology-Enhanced Orthopedic Materials*, 97–120, doi:10.1016/b978-0-85709-844-3.00005-7,(2015).
61. <http://theor.jinr.ru/disorder/carbon.html>
62. Petr Slepicka, Tomas Hubacek, Zdenka Kolska, Simona Trostova, Nikola Slepickova Kasalkova, Lucie Bacakova and Vaclav Svorečík, The properties and applications of carbon nanostructure, *Polymer science*,(2010)
63. Chris Binns, *Carbon Nanostructures: Bucky Balls and Nanotubes, Introduction to Nanoscience and Nanotechnology*,(2010)
64. Nanocarbon, *Fundamentals and Applications of Nano Silicon in Plasmonics and Fullerenes*, 287–309. doi:10.1016/b978-0-323-48057-4.00010-4,(2008).

65. Poole-Owens and Wolf, carbon nanostructures, Introduction to Nanoscience, Springer handbook,(2005)
66. T.C. Dinadayalane and J. Leszczynski, Fundamental Structural, Electronic, and Chemical Properties of Carbon Nanostructures: Graphene, Fullerenes, Carbon Nanotubes, and Their Derivatives, Handbook of Computational Chemistry,(2016)
67. Shenderova O. A, Zhirnov, V. V and Brenner D. W, Carbon Nanostructures. Critical Reviews in Solid State and Materials Sciences, 27(3-4), 227–356.doi:10.1080/1040843020850049,(2002).
68. Luis E. F. Foa Torres, Stephan Roche and Jean-Christophe Charlier, Introduction to Graphene-Based Nanomaterials: From Electronic Structure to Quantum Transport, Cambridge University Press, 978-1-107-03083-1, (2014)
69. Rafael Gregorio Mendes, Paweł S. Wróbel, Alicja Bachmatiuk, Jingyu Sun, Thomas Gemming, Zhongfan Liu and Mark Hermann Rummeli, Carbon Nanostructures as a Multi-Functional Platform for Sensing Applications , Chemosensors, 6, 60,(2018)